Journal of Membrane Science & Technology

Donose et al., J Membra Sci Technol 2016, 6:4
DOI: 10.4172/2155-9589.1000163

Research Article Open Access

Insight in to the Initial Stages of Silica Scaling Employing a Scanning Electron and Atomic Force Microscopy Approach

Bogdan C Donose*, Greg Birkett and Steven Pratt

The University of Queensland, School of Chemical Engineering, St Lucia, 4072, QLD, Australia

Abstract

The performance of reverse osmosis (RO) desalination can be limited by membrane scaling. Of particular concern is silica scale, which once deposited on the membrane is extremely difficult to remove. In this work, the deposition of silica-rich nanoparticles was considered. A novel *in situ* sample preparation method was developed for a microscopy investigation into the deposition and adhesion of the silica-rich nanoparticles. The method involves placing a clean silica wafer in agitated brine to collect particles to simulate initial stages of scaling. The 'scaled' surfaces were characterized by scanning electron microscopy (SEM) and atomic force microscopy (AFM). Model brines, with varying nanoparticle, cation, and organic composition and concentration were tested, as well as reject brine from a full-scale operational water treatment facility.

Microscopy revealed that silica-rich nanoparticles were deposited from all waters, with smaller nanoparticles more readily attaching to the wafer compared to larger ones. The presence of organics increased nanoparticle adhesion whereas divalent cations (Ca^{2+} and Mg^{2+}) decreased nanoparticle adhesion. These results have implications for the evaluation, selection and operation of RO pre-treatment processes and chemical dosing strategies, particularly the requirement for weak acid cation ion exchange (WAC-IX) and anti-scalant chemicals, respectively.

Keywords: Reverse osmosis; Brine; Silica; Scaling; Colloids; Electron and atomic force microscopy

Introduction

Reliable, safe and cost effective operation of reverse osmosis (RO) membrane desalination technology is vital to support development activities, urban and potable water supplies and agricultural activities in many parts of the world. In Australia, for example, the development of natural gas from coal seams offers tremendous economic opportunity, with development generating brackish 'produced water' which operators can manage using reverse osmosis (RO) membrane desalination to treat water to a quality suitable for a range of beneficial reuse such as agriculture. A waste brine stream is generated during the treatment process which requires storage and further treatment, management and subsequent disposal. A key operational objective can be to maximize the recovery ratio of the plant so to minimize the volume of brine requiring storage prior to, or during, treatment and disposal. The performance of the RO plants can be limited by silica derived membrane scale, which can be difficult to remove. Scaling is a common operational issue with RO membranes as documented in extensive academic and industry literature [1-6]. Groundwaters, including produced waters, are a complex matrix containing silica, hardness ions (e.g. calcium and magnesium), organics and other metal ions, with concentrations varying widely across regions. Our research group has recently shown that produced water has significant concentrations of silica-rich nanoparticles [7,8] and nanoparticles have been shown in the literature to have an adverse impact on the performance of membrane desalination [9-15]. A challenge in understanding the scaling mechanisms is the relatively slow kinetic of the process. Characterisation normally requires long-term experiments to make macro-scale observations. For this reason a new methodology was developed to quickly assess interactions between nanoparticles and membrane surfaces.

The interplay between silica-rich nanoparticles and the other components of produced water is not well understood. For example, experiments [10] have shown that the membrane flux decline during combined scaling and biofouling depends on solution chemistry and colloidal particle size. The combined fouling behaviour cannot be extrapolated from fouling by colloidal materials or dissolved organic matter alone. Synergistic effects were also found in fouling tests combining extracellular polymeric substances extracted from Pseudomonas aeruginosa PAO-1 and calcium ions [16]. These synergistic effects make selection and operation of infrastructure to mitigate scaling very challenging. For example, current literature-supported practice is to have weak acid cation exchange (WAC-IX) before the RO unit to reduce hardness in the RO feed stream. Some operations in the natural gas industry in Queensland (Australia) report that WAC IX operation has increased the frequency of RO membrane scaling events, with irreversible silica scale formation observed on RO membranes. Other operators have used IX without incident to the membranes but it is not clear if this operation is optimal.

In this work a novel *in situ* sample preparation method was developed for use with atomic force and electron microscopy to investigate the deposition and adhesion of silica-rich nanoparticles. The method simulates the initial stages of silica scale formation, whereby nanoparticles bind to silica-rich nanoparticles that are caught on membrane surfaces. The application of the method is demonstrated accompanied by a preliminary assessment of water matrix effects on particle adhesion. Synthetic produced water (with varying nanoparticle,

***Corresponding author:** Bogdan C Donose, The University of Queensland, School of Chemical Engineering, StLucia, 4072, QLD, Australia, Tel:+61(0)413286311; E-mail: b.donose@uq.edu.au

Received September 04, 2016; **Accepted** November 01, 2016; **Published** November 08, 2016

Citation: Donose BC, Birkett G, Pratt S (2016) Insight in to the Initial Stages of Silica Scaling Employing a Scanning Electron and Atomic Force Microscopy Approach. J Membra Sci Technol 6: 163. doi:10.4172/2155-9589.1000163

cation and organic content and composition) and brine from an operational reverse osmosis desalination facility are tested.

Materials and Methods

The experimental program involves depositing nanoparticles that are present in water samples on to silicon wafers (the silica trap), and then microscopy examination of the silicon wafers to assess the extent of deposition.

Silica trap

Silicon wafers (coated with a naturally grown silica layer of 2-4 nm) were diced (5×5 mm), washed in 10% H_2SO_4, rinsed in ethanol and de-ionised (DI) water and then cleaned (30 minutes) using a UV/Ozone unit (BioForce).

The wafers were immersed in the water samples in individual 50 ml plastic beakers for 24 hours under constant agitation (250 rpm) on an orbital shaker. After this step, the wafers were removed from the plastic beakers and immersed in DI water to rinse. Excess water was then removed from their surface using the corner of an extra low lint Kimwipes and wafers were placed in a vacuum oven for 8 hours at 70°C. Samples were stored in a high vacuum cabinet prior to mounting and SEM/AFM analysis. All steps undertaken for sample preparation and analysis are schematically presented in Figure 1.

Water samples

Table 1 summarises the types of water that were analyzed. Brine samples from a produced water RO desalination facility were typically collected on-site for the characterization of chemical composition. Water is separated from the natural gas at the well site and sent to the water management facility. The produced water then undergoes microfiltration followed by RO desalination.

Physical and chemical characterization of silica and other potential scalants were conducted using various spectroscopic and analytical techniques. Historical water quality data obtained from the RO desalination facility was used to generate an overview for a period of seven years. The RO process operates at around 80% recovery, generating a brine stream which is about 5 times as concentrated when compared to the RO feed. The water quality data of RO feed and brine

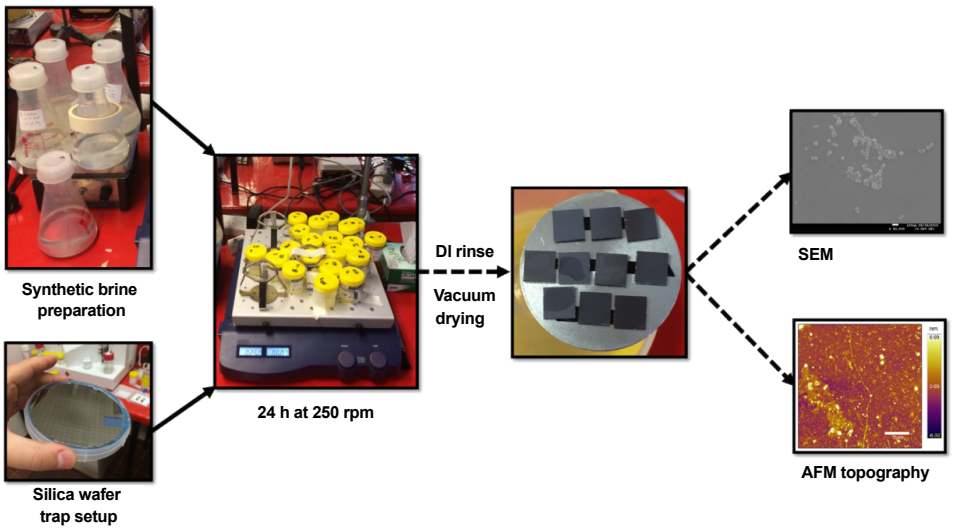

Figure 1: Silica trap experimental setup and preparation/analysis steps.

Experiment	Type of water	Characteristics
1	Model RO feed	pH, cations, organic surrogate, nanoparticles
2	Model brine	pH, cations, organic surrogate, nanoparticles
3	Real brine	Water matrix

Table 1: Waters tested employing silica trap method and their characteristics.

Measurement	Unit	RO feed		Brine		Conc. factor factor
		Average	St. dev.	Average	St. dev.	
Alkalinity (carb.)	mg/L	197.7	61.0	543.8	155.7	2.7
Calcium	mg/L	9.0	4.1	45.4	10.0	5.0
Magnesium	mg/L	2.5	1.2	13.1	2.5	5.2
pH	-	9.0	0.1	8.7	0.1	-
Potassium	mg/L	16.8	9.7	83.2	25.4	4.9
Silicon	mg/L	20.6	10.1	48.5	16.1	2.3
Sodium	mg/L	2557.8	877.4	12644.0	2062.4	4.9
TDS	mg/L	6565.5	677.5	27519.6	4281.8	4.1
TOC	mg/L	9.5	10.6	40.0	26.4	4.2

Table 2: Overview of RO feed and brine matrix profile.

is shown in Table 2. This shows that the produced water is rich in sodium and bicarbonate, with potassium, calcium, and magnesium also present. The silica concentration in the produced water feed is relatively low, but the recovery process increases the silica concentration to near saturation. Such a concentration increase can lead to a dramatic change in the silica particulate fraction: before RO approx. 7% and after RO approx. 35% [7].

Synthetic produced waters, RO feed and brine, were prepared using DI water produced by a Millipore Academic unit (resistivity lower than 18 MΩ·cm), silica nanoparticle standards (Sigma, Ludox 12 nm in diameter and Nissan chemical, Snowtex ST-20L, 60 nm in diameter). $CaCO_3$, K_2CO_3, $MgSO_4$, NaCl were of analytical grade and were used without prior purification. 1.0 M HCl and 1.0 M NaOH were used for pH adjustment.

Using the historical RO desalination facility data as a guide, two types of synthetic waters were used: brine and produced water feed. Concentration factors of 5 were imposed for all ions. Considering silicon is present as dissolved and particulate silica, a concentration factor of 25 for silicon was chosen to cover the observed ranges of particulate and dissolved Si, i.e. to account for a fivefold increase in silica particulate fraction seconded by a silicon concentration factor of five. In this way the chance to observe attached nanoparticles by microscopy techniques was increased.

Table 3 shows the program for the model RO feed and model brine experiments. The table shows the types of samples used in this study as well as the pH values of the synthetic waters in which silica wafer traps were immersed. The conditions tested were: presence or absence of silica nanoparticles or dissolved silica (leftmost columns in Table 4) and different combinations of hardness ions, organics surrogate in deionised water (top row). As silica surrogates, Ludox (diameter=12 nm), Snowtex (diameter=60 nm) and dissolved silica in HF were employed.

The real brine samples were treated in the same manner for microscopy analysis.

Scanning electron microscopy (SEM) and atomic force microscopy (AFM)

SEM was performed by employing a JEOL 7001 Field Emission Gun at 10 mm working distance, spot size 8 or 9 and 5 kV-10 kV accelerating voltage.

AFM micrographs were recorded employing an MFP-3D built on an Eclipse Ti-U Nikon inverted microscope, placed on a Herzan anti-vibration table which was housed in a TMC enclosure and a Cypher (Asylum Research/Oxford Instruments) using Multi 75 DLC (Budget Sensors, Bulgaria) probes of nominal contact radius less than 15 nm and nominal spring constant of 2 N/m. All samples were imaged at 0.7-1 Hz scan rate in AC mode in air over an area of 2×1 μm.

For both microscopy methods samples were imaged as received, post vacuum deposition (as described in above in 2.1 Silica trap), in order to prevent interference potentially introduced by a conductive layer. In this way the errors of scanning are limited only to accelerating voltage and spot size (for SEM) and probe contact radius (for AFM).

Results and Discussion

Experiment 1: Model RO feed

SEM and AFM micrographs for synthetic RO feed produced water are presented in Figures 2 and 3. Both microscopy techniques confirm that nanoparticles were trapped on the wafer. All samples exhibit adhered structures. Several features are captured by SEM at a larger scale, allowing for a general sample overview, while AFM reveals more three-dimensional details. These features include alginate networks (AFM NO-1), salt crystals (SEM NO-3) and nanocrystals (AFM LU-4), as well as nanoparticles (SEM SN-1, AFM SN-4).

As described in the experimental section, after exposure to the water sample under constant agitation, wafers are rinsed with DI water, the excess water is removed and then subjected to thermally assisted

Ion	Model RO feed(mg/L)	Model brine (mg/L)
Na^+	2200	11400
Mg^{2+}	2	10
Ca^{2+}	8	40
CO_3^{2-}	72	36
K^+	39	183
SO_4^{2-}	9	48
Si^{4+}	4	100
Alginate	20	100

Table 3: Model brine and RO feed water matrices (with all ions present).

Model feed	Na mg/L	Ca mg/L	Mg mg/L	Alg mg/L	Silica nanoparticles and pH			
					NO	ST	LU	SN
1	2200	8	2	20	8.2	8.8	8.7	8.7
2	2200	8	2	-	8.6	8.9	8.9	8.5
3	2200	-	-	20	8.9	8.9	8.9	8.9
4	2200	-	-	-	8.0	8.9	9.0	8.2
5	-	-	-	-	8.7	8.7	8.8	8.9
Model brine								
1	11400	40	10	100	8.5	8.6	8.6	8.9
2	11400	40	10	-	8.5	8.6	8.5	8.7
3	11400	-	-	100	8.8	8.8	8.5	8.8
4	11400	-	-	-	8.8	8.8	8.5	8.9
5	-	-	-	-	8.7	8.7	8.9	8.7
				TOC (mg/L)	**Si** (mg/L)		**pH**	
Real feed	2557.8	9.0	2.5	9.5	20.6		9	
Real brine	12644.0	45.4	13.1	40.0	48.5		8.7	

Table 4: Sample matrix and pH for synthetic and real waters. Sample codes: NO=no silica; ST=dissolved silica; LU=Ludox silica; SN=Snowtex. The numbered columns and labels show the presence/absence of major ions in solution.

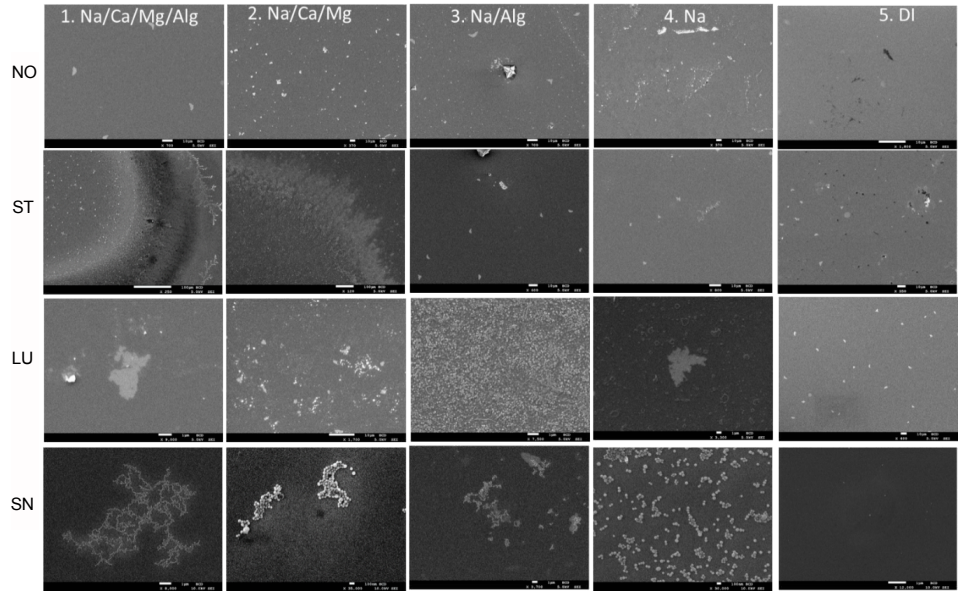

Figure 2: Representative SEM micrographs of the wafer surfaces after exposure to synthetic RO feed waters and selected features marked by red arrows (Scale bars: NO-1 to NO-5, 10 µm; ST-1 and 2, 100 µm; ST-3 to 5, 10 µm; LU-1, 3 and 4, 1 µm; LU-2 and 5, 10 µm; SN-1, 3 and SN5, 1 µm; SN-2 and 4, 100 nm.

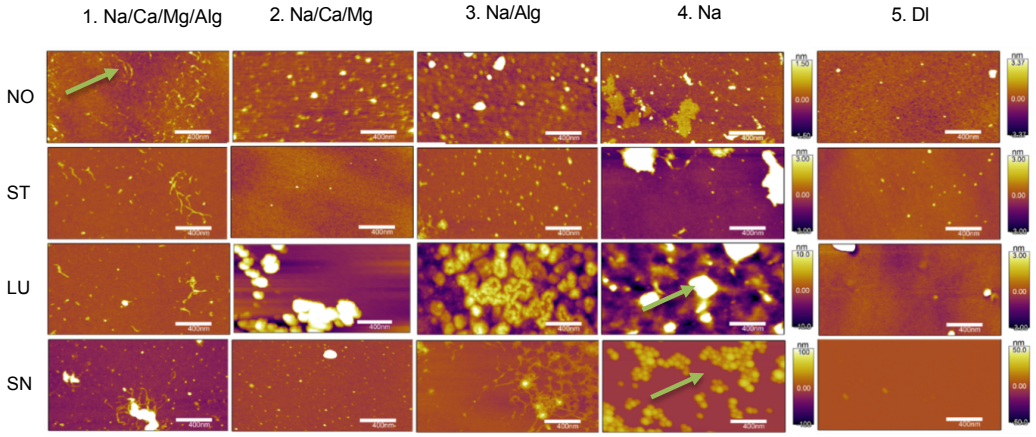

Figure 3: Representative AFM micrographs of the wafer surfaces after exposure to synthetic RO feed waters and selected features marked by green arrows (Scale bars: 400 nm): NO-1: dendritic structures; LU-4: large salt crystals; SN 4: isolated NPs clusters.

vacuum drying. This approach poses significant challenges in choosing a representative area for analysis, especially when samples exhibit salt drying patterns leading to imaging artefacts such as in SEM ST-1 and SEM ST-2 (Figure 2).

In the presence of cations and alginate the dendritic alginate structures (from AFM) and aggregates with colloids (SEM and AFM) are apparent (Figures 2 and 3: column 1. Na/Ca/Mg/Alg). When alginate is removed (column 2. Na/Ca/Mg) the dendritic structures disappear and patches of aggregates can be observed. Removing the divalent cations (column 3. Na/Alg) results in a compact multilayered mat of Ludox nanoparticles being deposited on the trap surface. It is also shown that SN nanoparticles exhibit a different behaviour, suggesting that smaller NPs are more easily attached to the surface. In the presence of just sodium (column 4. Na) different attachment behaviour between SN and LU NPs was observed, with smaller particles attaching more readily. The benchmark (column 5. DI water) confirms little or no attachment as result of electrostatic repulsion.

Experiment 2: Model brine

SEM and AFM micrographs for synthetic brine are presented in Figures 4 and 5. Similar to the case of model RO feed, both microscopy techniques confirm that the trapping approach was successful. For the model brine the adhered structures were more abundant. This was expected because concentration of ions in the brine was increased by a factor of 5 compared to the RO feed, except for silicon which was increased by a factor of 25 to reach 100 mg/L. Again, the observed features included alginate networks (AFM NO-1), salt crystals (SEM NO-3) and nanocrystals (SEM NO-4), as well as nanoparticle dense mats (SEM SN-4, AFM SN-4).

Differences in the adhesion of nanoparticles are most pronounced when comparing both SEM and AFM for the LU4 and SN4 samples. The larger Snowtex particles form layers with voids, while Ludox mats are compact and possibly multi layered. Even at high silicon

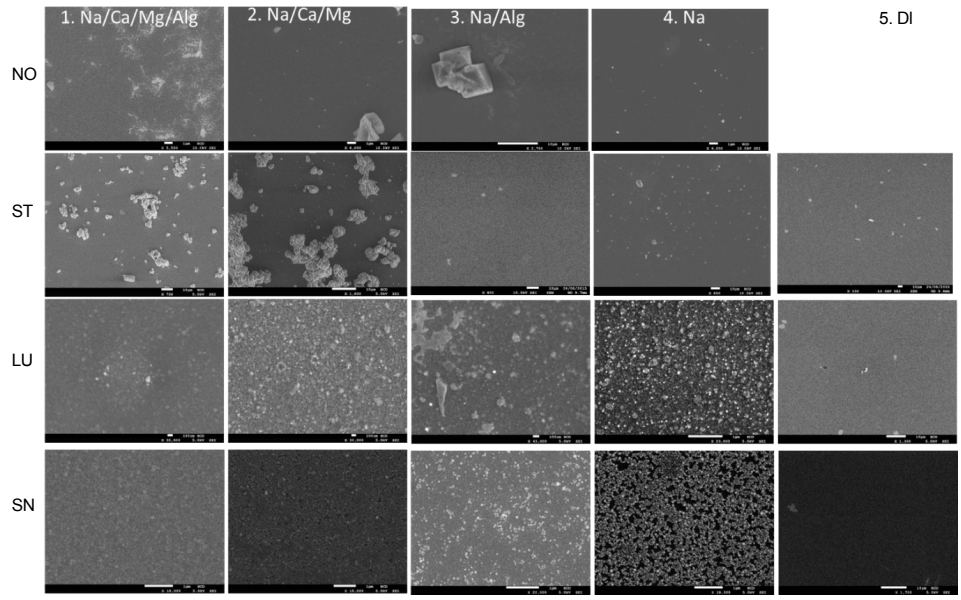

Figure 4: Representative SEM micrographs of the wafer surfaces after exposure to synthetic brine waters and selected features marked by red arrows (Scale bars: NO-1, 2 and 4, 1 µm; NO-3, 10 µm; ST-1 to 5, 10 µm; LU-1 to 3, 100 nm; LU-4, 1 µm; LU-5, 10 µm; SN-1 to 4, 1 µm; SN-5, 10 µm).

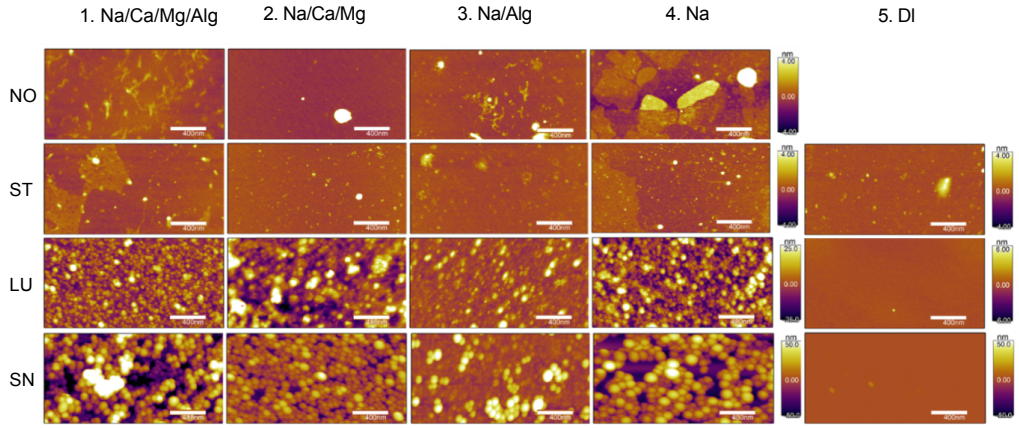

Figure 5: Representative AFM micrographs of the wafer surfaces after exposure to synthetic brine waters and selected features marked by green arrows: NO-1 dendritic structures; SN-4 voids in the Snowtex layer.

concentrations (100 mg/L) benchmark tests with DI water show again a total lack of adhesion due to electrostatic repulsion.

A summary of distinguishing features observed on all samples is presented in Table 5.

Experiment 3: Real brine

Microfiltered brine from a RO desalination facility was also considered. Data is presented in Figure 6, along with, for comparison, traps exposed to synthetic produced waters containing all ionic components and grouped as: no silica, standard dissolved silica, Ludox nanoparticles and Snowtex nanoparticles.

The figure shows that traps exposed to microfiltered brine exhibit a combination of all surface elements presented on the traps from the model waters: dendritic structures (squares), colloidal aggregates (triangles) and salt crystals (circles). The topographical differences between RO feed and brine in samples containing all the ingredients (mono and divalent cations and organic surrogate/alginate) are highlighted.

There are three types of effects emerging from the existing data:

1. Colloids size is a determining factor in deposition and aggregation as visualised in synthetic brine, with Ludox, the smallest colloids, being easily attached and forming multilayered colloidal mats in comparison with Snowtex which attached as loose monolayers.

2. The presence of alginate (as surrogate for organic matter) in the matrix contributes to an enhancement of colloids/particulates attachment and aggregation.

3. When cations are removed from the RO feed an enhancement of silica deposition on the trap wafer is observed in model feed water.

Discussion

As previously postulated [17], the adhesion between solid particles

Model feed	1 Na/Ca/Mg/Alg	2 Na/Ca/Mg	3 Na/Alg	4 Na	5. pH adjusted DI water
NO (without silica)	Alg. network	Salt nanocrystals	Alg. networks and colloids	-	Clear surface
ST (dissolved silica)	Alg. islands	Clear surface	Alg. network and nanocrystals	-	Few colloids
LU (Ludox nanoparticles)	Alg. network	Large crystals	Colloids mat	Colloids mat	Clear surface
SN (Snowtex nanoparticles)	Colloids and alg. networks	Isolated colloids	Isolated alg. embedded colloids	Dispersed colloids	Clear surface
Model brine	**1**	**2**	**3**	**4**	**5**
NO (without silica)	Alg. network	-	Alg. network &colloids	Salt crystals	Clear surface
ST (dissolved silica)	Silica and alginate islands	Aggregates	Alginate network and colloids	Crystals and colloids	Colloids and aggregates
LU (Ludox nanoparticles)	Colloids dense mat	Colloids mat and aggregates	Alginate embedded colloids and islands	Colloids mat &aggregates	Clear surface
SN (Snowtex nanoparticles)	Colloids loose multilayer	Colloids loose layer and aggregates	Alginate embedded colloids	Colloids loose layer	Clear surface

Table 5: Sample matrix and distinguishing features on traps exposed to synthetic RO feed and brine.

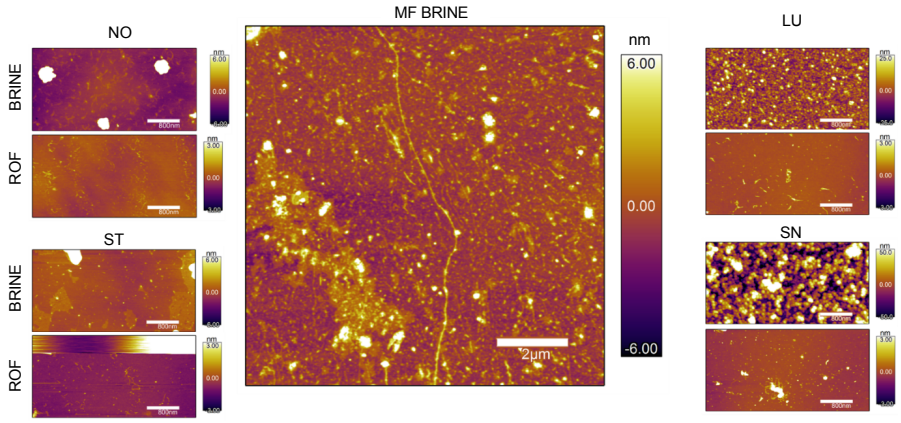

Figure 6: AFM comparison (to scale in XY coordinates) between surfaces exposed to real WTF micro-filtered brine and synthetic (1: Na/Ca/Mg/Alg) waters: no silica, standard silica, Ludox and Snowtex. Marked features: dendritic structures (squares), colloidal aggregates (triangles) and salt crystals (circles).

and solid surfaces is determined by van der Waals, electrostatic and deformational forces [18]. For particles in the nanoscale domain the long range electrostatic force becomes less important and van der Waals, structural and hydration forces dominate interaction and challenge to the limit existing analytical tools such as surface force apparatus and AFM. Over the recent decades of nanoscale force measurements, silica and mica surfaces were tested typically in electrolyte solutions of controlled pH and salt concentration to learn how van der Waals, adhesion, solvation, structural and friction forces behave [19-27]. To our knowledge, there is no comprehensive model that describes interactions in complex fluids such as brines resulting from water treatment. In an experimental system such as the one designed and analysed here, as a proxy to the brine or pre-brine medium, the roughness of the substrate was chosen on purpose to be at its minimum in order to reduce its contribution. The propensity of smaller nanoparticles to attach to the smooth silica could be attributed to the increasing role of van der Waals interactions and to the reduced hydrodynamic effect acting synergistically toward immobilising very small colloids.

The role of alginate in the enhanced colloid/particulates attachment has been previously tested [28] in high ionic strength environments to show that the polyelectrolyte nature of alginate reduces steric repulsion and favours adhesion. Similarly, its ability to enhance adhesion has been harnessed to boost the impact and efficiency of drug delivery systems [29]. In certain experimental conditions [30,31] alginate was shown to be able to restore flux in fouled membranes, based on its ability to interact with silica.

Without having a definitive answer with regard to the effect of the absence of cations on the silica deposition, namely an increasing amount of deposited colloids, this behaviour could be linked to the ability of certain cations to reduce friction between silica surfaces [21,22]. Also, the role of pH, needs to be further assessed, especially in the vicinity of pH 9 [25] where silica has an accelerated dissolution rate and where hydration and hydrogen bonding and depolymerisation play such an important role.

Conclusions

Silica wafer samples prepared by immersion for 24 hours (under constant agitation) in different types of water are suitable to trap nanoparticles, nanocrystals and organic dendritic structures and their aggregates, which later on, can be subjected to microscopy. Considering silica-silica interactions in different media, the new method allows taking snapshots of the early stages of scaling, replacing a rough RO polyamide substrate [31] by a flat wafer (roughness less than 1 nm as measured by AFM), more suitable for SEM and AFM. The

combination of two microscopies and samples' preparation enables obtaining information which otherwise would be inaccessible.

Acknowledgements

This research is supported and funded by the UQ Centre for Coal Seam Gas, which includes industry members APLNG, Arrow Energy, QGC and Santos Ltd. Deirdre Walsh, Paul Wybrew and Josh Davies are acknowledged for reviewing the manuscript. This work was performed in part at the Queensland node of the Australian National Fabrication Facility, a company established under the National Collaborative Research Infrastructure Strategy to provide nano and micro-fabrication facilities for Australia's researchers. The authors acknowledge the facilities and the scientific and technical assistance of the Australian Microscopy & Microanalysis Research Facility at the Centre for Microscopy and Microanalysis (The University of Queensland).

References

1. Antony A, Low JH, Gray S, Leslie G (2011) Scale formation and control in high pressure membrane water treatment systems: A review. J Mem Sci 383: 1-16.
2. Duong HC, Gray S, Duke M, Nghiem L (2015) Scaling control during membrane distillation of coal seam gas reverse osmosis brine. J Mem Sci 493: 673-682.
3. Sheikholeslami R, Tan S (1999) Effects of water duality on silica fouling of desalination plants. Desalination 126: 267-280.
4. Butt FH, Rahman F, Baduruthamal U (1995) Pilot plant evaluation of advanced vs conventional scale inhibitors for RO desalination. Desalination 103: 189-198.
5. Butt FH, Rahman F, Baduruthamal U (1995) Identification of Scale Deposits through Membrane Autopsy. Desalination 101: 219-230.
6. Butt FH, Rahman F, Baduruthamal U (1997) Characterization of foulants by autopsy of RO desalination membranes. Desalination 114: 51-64.
7. Zaman M, Birkett G, Pratt C, Stuart B, Pratt S (2015) Downstream processing of reverse osmosis brine: Characterisation of potential scaling compounds. Water Res 80: 227-234.
8. Zaman M, Masuduz, Greg B, Stuart B, Pratt S (2013) Silica Removal from Coal Seam Gas Brine Using Activated Alumina, in CHEMECA: Australasian Conference on Chemica Engineering pp: 700-703.
9. Fang Y, Duranceau S (2013) Study of the Effect of Nanoparticles and Surface Morphology on Reverse Osmosis and Nanofiltration Membrane Productivity. Membranes 3: 196-225.
10. Li QL, Elimelech M (2006) Synergistic effects in combined fouling of a loose nanofiltration membrane by colloidal materials and natural organic matter. J Mem Sci 278: 72-82.
11. Park JY, Lim S, Park K (2013) A new approach for determination of fouling potential by colloidal nanoparticles during reverse osmosis (RO) membrane filtration of seawater. J Nanopart Res 15: 1548.
12. Zhu X, Elimelech M (1997) Colloidal Fouling of Reverse Osmosis Membranes: Measurements and Fouling Mechanisms. Environ Sci Technol 31: 3654-3662.
13. Belfort G, Davis RH, Zydney AL (1994) The Behavior of Suspensions and Macromolecular Solutions in Cross-Flow Microfiltration. J Mem Sci 96: 1-58.
14. Faibish RS, Elimelech M, Cohen Y (1998) Effect of interparticle electrostatic double layer interactions on permeate flux decline in crossflow membrane filtration of colloidal suspensions: An experimental investigation. J Colloid Interface Sci 204: 77-86.
15. Fane AG, Fell CJD (1987) A Review of Fouling and Fouling Control in Ultrafiltration. Desalination 62: 117-136.
16. Herzberg M, Kang S, Elimelech M (2009) Role of Extracellular Polymeric Substances (EPS) in Biofouling of Reverse Osmosis Membranes. Environ Sci Technol 43: 4393-4398.
17. Chow TS (2003) Size-dependent adhesion of nanoparticles on rough substrates. J Phys Condens Matter 15: L83-L87.
18. Israelachvili JN (2011) Adhesion and Wetting Phenomena, in Intermolecular and Surface Forces. Third Edition, Academic Press: San Diego pp: 415-467.
19. Vakarelski IU, Ishimura K, Higashitani K (2000) Adhesion between Silica Particle and Mica Surfaces in Water and Electrolyte Solutions. J Colloid Interface Sci 227: 111-118.
20. Donose BC, Taran E, Vakarelski IU, Shinto H, Higashitani K (2006) Effects of cleaning procedures of silica wafers on their friction characteristics. J Colloid Interface Sci 299: 233-237.
21. Donose BC, Vakarelski IU, Higashitani K (2005) Silica surfaces lubrication by hydrated cations adsorption from electrolyte solutions. Langmuir 21: 1834-1839.
22. Donose BC, Vakarelski IU, Taran E, Shinto H, Higashitani K (2006) Specific effects of divalent cation nitrates on the nanotribology of silica surfaces. Ind Eng Chem Res 45: 7035-7041.
23. Ducker WA, Senden TJ, Pashley RM (1991) Direct Measurement of Colloidal Forces Using an Atomic Force Microscope. Nature 353: 239-241.
24. Hampton MA, Donose BC, Taran E, Nguyen AV (2009) Effect of nanobubbles on friction forces between hydrophobic surfaces in water. J Colloid Interface Sci 329: 202-207.
25. Taran E, Donose BC, Vakarelski IU, Higashitani K (2006) pH dependence of friction forces between silica surfaces in solutions. J Colloid Interface Sci 297: 199-203.
26. Biggs S, Cain R, Page NW (2000) Lateral Force Microscopy Study of the Friction between Silica Surfaces. J Colloid Interface Sci 232: 133-140.
27. Raviv U, Klein J (2002) Fluidity of Bound Hydration Layers. Science 297: 1540-1543.
28. De Kerchove AJ, Elimelech M (2007) Impact of Alginate Conditioning Film on Deposition Kinetics of Motile and Nonmotile Pseudomonas aeruginosa Strains. Appl Environ Microbiol 73: 5227-5234.
29. Hu L, Sun C, Song A, Zheng X, Chang D, et al. (2014) Alginate encapsulated mesoporous silica nanospheres as a sustained drug delivery system for the poorly water-soluble drug indomethacin. Asian J Pharm Sci 9: 183-190.
30. Higgin R, Howe KJ, Mayer TM (2010) Synergistic behavior between silica and alginate: Novel approach for removing silica scale from RO membranes. Desalination 250: 76-81.
31. Donose BC, Subhash S, Marc P, Yvan P, Jurg K, et al. (2013) Effect of pH on the ageing of reverse osmosis membranes upon exposure to hypochlorite. Desalination 309: 97-105.